

MR ANGIOGRAPHY, FLOW, AND ENDOTHELIAL FUNCTION

High-field MR angiography on an in vitro stenosis model determination of the spatial resolution on 1.5 and 3T in correlation to flow velocity and contrast medium concentration

T. WITTLINGER,^{1,*} I. MARTINOVIC,¹ R. NOESKE,² R. MOOSDORF,¹ and F. LEHMANN³

¹Department of Heart Surgery, University Hospital, Marburg, Germany

²GE Medical Systems, Freiburg, Germany

³Institute of Informatics, Biometry and Epidemiology, University of Essen, Essen, Germany

Since the first description of coronary magnetic angiography (MRA) in the early of 1990, this method seems to be shaped as a promising noninvasive modality to view the coronary arteries. Since several years dedicated high-field MR systems up to 4T are available for human use. The aim of the study was the evaluation of an in vitro vessel model with defined stenoses on 1.5T and 3T. For imaging at 3T, we used a 3d gradient-echo-sequence (fast SPGR). Furthermore, we examined the influence of the flow velocity and the contrast medium concentration on the spatial resolution. The accurate detection of in vitro stenoses was possible in segments up to 0.6 mm at 3T, the best results were obtained at a flow velocity of 40 ml/min and a contrast medium concentration of 0.2 mmol/l. The influence of the contrast medium concentration was statistically not significant. These results show that the spatial resolution can be increased by the use of a high-field MR scanner. Further in vivo studies are necessary to eliminate the method's limitation in visualizing small distal vessel segments.

Key Words: Magnetic resonance coronary angiography; High-field magnetic resonance tomography; Coronary artery imaging; In vitro coronary angiography; 3T

1. Introduction

The non-invasive imaging of coronary vessels has been possible for some years using the method of magnetic resonance imaging (MRI) (1–6).

The image resolution in conventional cardiac catheterization tests is in the region of 300 μm (7). Such a high spatial resolution can, in principle, also be achieved by means of MRI. Despite many new technical advances in different imaging methods, the ability to visualize and assess further distal located branches and small vessels is desirable and quantitative grading of coronary artery stenosis is the ultimate goal.

Currently, the use of new sequences such as “steady-state free precession,” black-blood coronary angiography or 3D spiral scanning to increase the contrast between blood and surrounding tissue shows much promise (7). The reliability with which stenosis of the coronary arteries are recognized, above all in the middle and distal segments, is currently the subject of intensive research in several multicenter studies (8).

Until 1998, high-field MR scanners with an output of 3T were solely used as research equipment, due to the lack of an FDA approval for use in patients (9). The extension of non-significant risk status for clinical fields up to 8T by the FDA in 2003 facilitates the further growth of this technology. Several studies have demonstrated no significant changes in vital signs in subjects exposed to field strength up to 8T (10).

Since 2003, two comparative studies at 1.5T and 3T have been published, which focused primarily on the signal-to-noise (SNR) and contrast-to-noise (CNR) ratios (11, 12).

The construction of appropriate receiver coils for cardiac imaging is one of the challenges posed by high-field equipment (13, 14). Together with the substantial increase in resonance frequency, there is also an rise in the amount of radiofrequency energy applied, which necessitates special strategies for imaging techniques since these already have a large energy deposition at 1.5T.

Potential disadvantages of the high-field MR method include susceptibility artefacts, small T_2^* and longer T_1 periods as well as radio frequency distortion (15). Advances in 3T hardware together with the development of more powerful magnets and special receiver coils as well as the use of T_2 -prep sequences and 2-D real-time navigators enabled 3T MRA. The first study on high-field 3T MR coronary angiography on healthy volunteers was published by Stuber et al. in 2002 (15).

Received 7 October 2004; accepted 19 April 2005.

*Address correspondence to Dr. med.Th. Wittlinger, Department of Thoracic and Cardiovascular Surgery, University Hospital, Theodor-Stern-Kai 7, D-60590 Frankfurt, Germany; Fax: 0049-(0)6732/65370; E-mail: thomaswittlinger@t-online.de

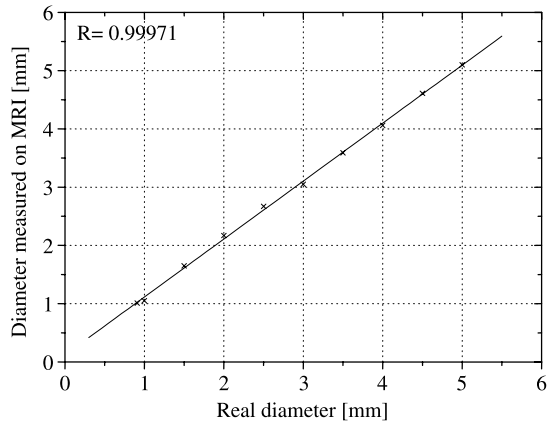


Figure 1. Determination of the diameter of stenosis in correlation with a reference value at a flow rate of 40 ml/min. A very good correlation with the non-invasively measured stenosis parameters is seen at 1.5 T.

Current limitation of MRA include a suboptimal signal-to-noise (SNR), which limits spatial resolution and the ability to visualize distal vessel segments < 1.5 mm. Improved SNR is expected at higher field strength, which may provide improved spatial resolution. At higher field strengths, there is, on the one hand, an associated gain in the signal-to-noise ratio, but this occurs at the cost of higher sensitivity to the negative effects of the static field and an altered relaxation time (9). This necessitates adjustments to the imaging techniques.

Therefore, the SNR can be favourably affected by a higher field strength of 3T. 3.0T imaging shows approximately a 2.0-fold increase in SNR over imaging at 1.5T (16). This improvement in image quality can be used to increase the in-plane-resolution down to a vessel diameter less than 1 mm (17).

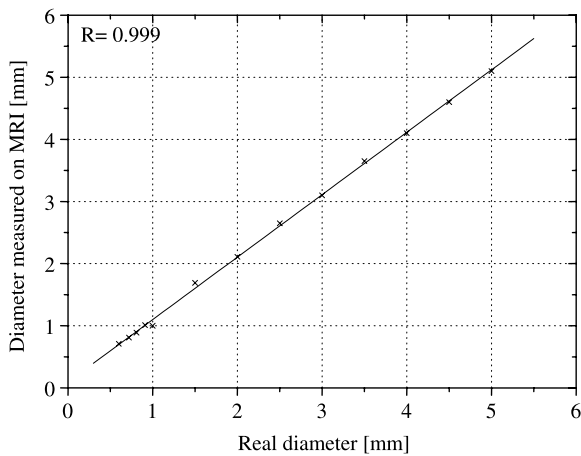


Figure 2. Determination of the diameter of stenosis in correlation with a reference value at a flow rate of 40 ml/min. A very good correlation with the non-invasively measured stenosis parameters is seen at 3 T.

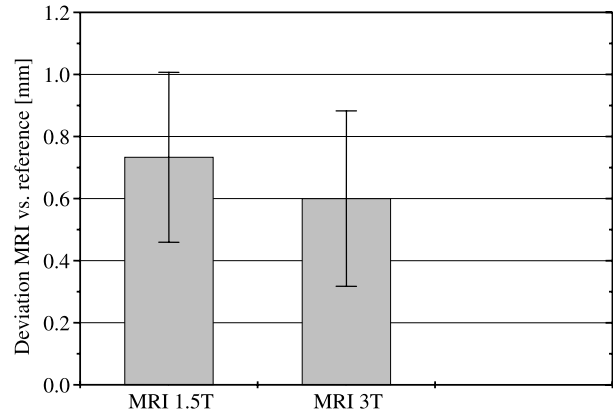


Figure 3. Estimation of the length of stenosis. It must be taken into consideration that in the 3T study more high-grade and short stenosis of < 5 mm in length will be included into the study and thus the variance will be greater.

Our first step was to investigate the efficiency of a 1.5 and 3T scanner with respect to the maximum spatial resolution in a defined in vitro vessel model. The effects of different contrast medium concentrations and flow rates were also investigated.

On the basis of knowledge derived from this study, further investigations are planned for native vessel preparations and also on healthy volunteers in the near future.

2. Methods

For the exact evaluation of the stenosis, we used a glass tube in vitro vessel model with defined diameter. The glass tubes were embedded in Plexiglas. The details are given in Tables 1 and 2.

The phantoms consisted of a 3×4 cm plexiglass block with glass tubes inlays. All of the stenosis models had an internal diameter of 2.8 mm, with the stenosed segments having a diameter between 0.3 and 2.5 mm, corresponding to

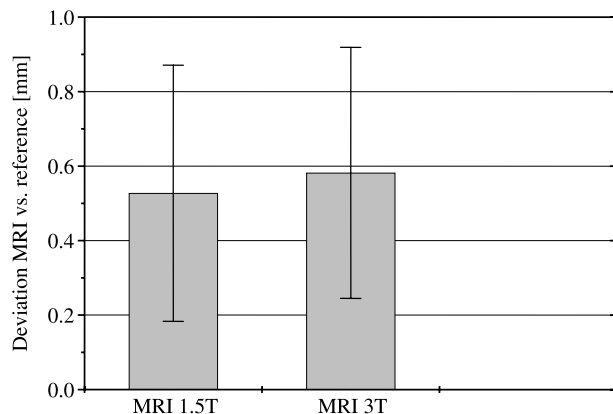


Figure 4. Estimation of the pre- and post-stenotic length ratio with 1.5 and 3 T.

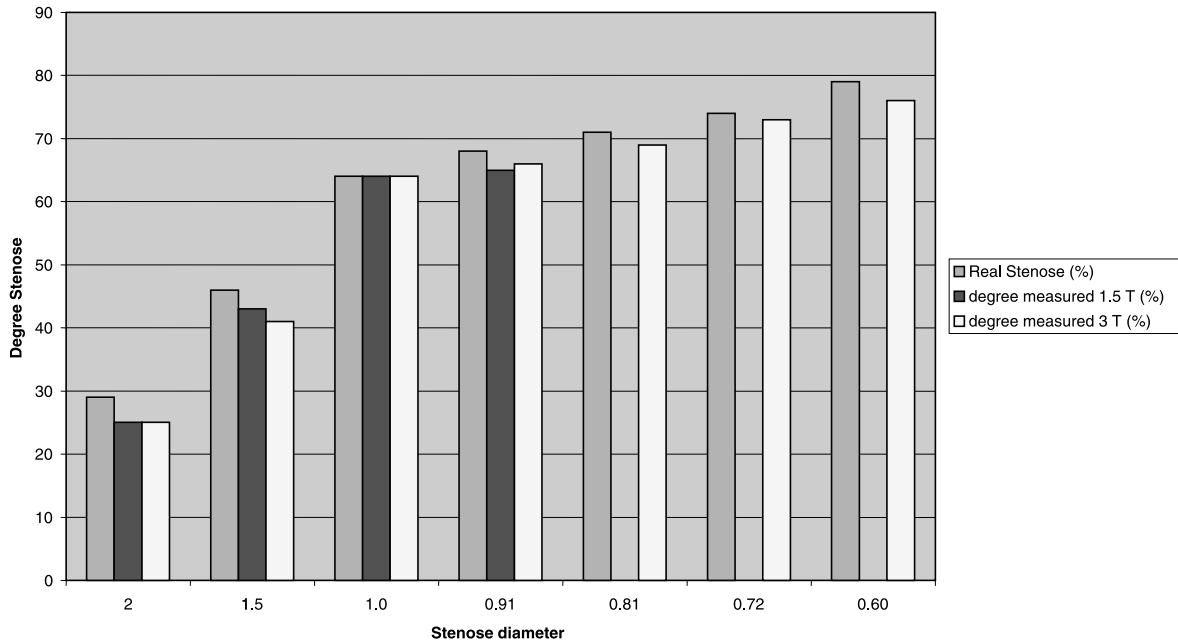


Figure 5. Assessment of the stenosis degree with 1.5 and 3 T in correlation to the real value.

stenosis of 11–90%. The lengths of the stenosis were 3–10 mm (Fig. 6). The non-stenosed models had a diameter of 3–5.5 mm (Table 2).

For imaging, we utilized a fluid with a susceptibility characteristic and with properties similar to those of blood. We used a gadopen-based contrast medium (Magnevist 0.5 mmol/ml, Schering AG, Berlin, Germany). In order to determine the influence of contrast medium concentration on spatial resolution, we perfused the models with Magnevist 0.1 mmol, 0.2 mmol, and 0.3 mmol.

The study was carried out with stationary contrast medium as well as with a defined flow rate. Flow rates of 40 and 60 mL/min with constant flow were used, which correspond to the average intracoronary flow rates as described in the literature (12) and also as determined in our own patient studies. Continuous flow rates were produced by means of a pump (Laudathermostat Typ GPS 1517, Dr. K Wobsa GmbH, Germany), which, on account of the ferromagnetic housing, was set up outside the MR area and was connected to the phantom by means of a sufficiently long supply line.

Table 1. Diameter non-stenotic models

Vessel diameter	3.0 mm	3.5 mm	4.0 mm	4.5 mm	5.0 mm	5.5 mm
-----------------	--------	--------	--------	--------	--------	--------

Table 2. Parameter stenotic models

Vessel diameter	Diameter stenosis	Degree/%	Length stenosis	Length pre-sten.	Length post-sten.
2.8	0.3	90	3	11	3
2.8	0.40	85	3	11	3
2.8	0.50	82	5	11	4
2.8	0.60	79	5	11	4
2.8	0.72	74	9	10	0
2.8	0.81	71	9	10	0
2.8	0.91	67	10	7	0
2.8	1.0	65	10	7	0
2.8	1.5	46	10	7	0
2.8	2.0	28	7	10	0
2.8	2.5	11	7	10	0

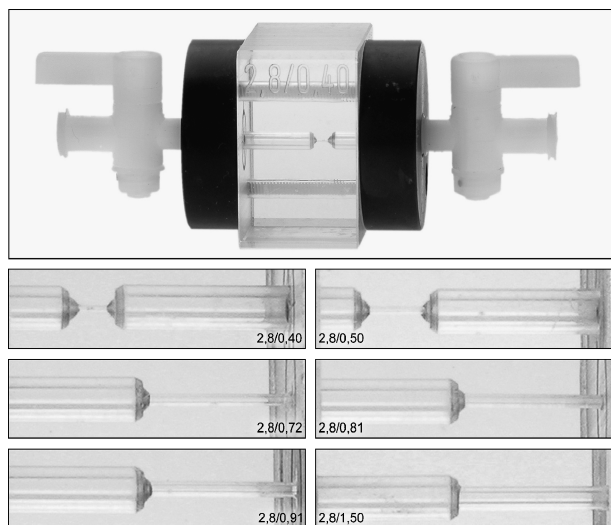


Figure 6. Model of the phantom with defined stenosis.

The flow rates set at the pump had been tested in a previous study using an electromagnetic flowmeter (Carolina Medical Electronics Inc, North Carolina, USA).

The phantom was placed into a water bath together with the supply line, in order to simulate an environment like that of the human thorax. The surrounding liquid consisted of 10% hydroxyethyl starch, which has a similar consistency to that of human tissue.

2.1. 1.5T MR imaging

Coronary in vitro MRI was performed on a whole body 1.5T Inera scanner (Philips Medical Systems, Best, The Netherlands) with a gradient of 30 mT and a slew rate of 150T/m/s. For signal acquisition, a multi-segment quadrature T/R head coil, for imaging a 3D T1 fast-field-echo gradient-echo-sequence (TE minimum, flip angle 25° , matrix 512×512 , FOV 30 cm, slice thickness 1 mm, 30 overlapping- slices) were used.

The total scan time was 52 seconds.

2.2. 3T MR imaging

The in vitro models were examined on a 3T MR scanner (Signa 3T, GE Medical Systems, Milwaukee, WI, USA) with a gradient of 40 mT, the rise time was 268 ms. The effective gradient amplitude was 69 mT/m, and the effective gradient slew rate was 259T/m/s.

The minimal slice thickness was 0.5 mm at the 2D acquisition and 0.1 mm at 3D. The minimal FOV was 10 mm, the maximal 400 mm.

The study was performed on both systems with a multi-segment quadrature T/R head. To use the same design and size as the 3T prototyp coil, the standard head coil was used at 1.5T instead of the smaller cardiac phased array coil.

The MRI was performed with 3D gradient-echo-sequences (fast SPGR, spoiled gradient echo) with a TE of minimum, flip angle of 25° , matrix of 512×512 , FOV 30 cm and a slice thickness of 1 mm.

The maximal TR was 2.9 ms, the minimal 0.9 ms.

The total scan time for Nex 0.5 was 52 seconds, for NEX 1 1 minute 12 seconds and for NEX 2 1 minute and 30 seconds.

In order to improve spatial resolution, we carried out measurements with NEX = 0.5, 1 and 2, where NEX stands for signal averaging. Thus, NEX = 0.5 represents a half Fourier transformation of the k space, whereby only slightly more than half of the lines of the k-space are selected, and the rest of the image is reconstructed from these data. NEX = 1 represents the standard transformation of the entire k space. With NEX = 2, two averages are taken, which makes it possible for an increase of about 40% to be achieved in the signal-to-noise ratio (Table 3).

2.3. Image analysis

The image analyses were performed on the 3D data on a VARIAN UNITY INOVA system.

For measurements, the image data were reformed in a multiplanar fashion as described previously (18).

The determination of the internal diameters was carried out at the workstation on the basis of the different measurements and with the help of a signal intensity profile using the technique described in the paper by Hoogeveen et al. (19).

2.4. Statistics

The reliability of the method was calculated using sensitivity and specificity tables.

Furthermore, the concordance correlation was determined using the method of Lin (20). This is + 1 when there is a perfect concordance.

The 95% confidence levels for sensitivity and specificity were calculated following an approximation according to the Geigy Scientific Tables (21).

At the 95% confidence level, the *P* value (McNemar's Test) and Cohen's kappa showed a correlation between experimental and reference groups as well as among members of the experimental groups.

The results of the flow measurements were investigated using the t-test and a value < 0.05 was considered to be statistically significant.

All calculations were carried out using SAS/Stat Version 8.2.

Table 3. TE and TR in correlation to NEX at 3 T

	NEX 0.5	NEX 1	NEX 2
TE	2.5	1.7	1.7
TR	7.0	6.2	6.2

3. Results

At 1.5T, vessel stenosis with a minimum diameter of 0.91 mm can be evaluated. MRI overestimates the actual diameters. The best results were obtained at a flow rate of 40 mL/min; however, the differences were not significant (Table 4). Determination of the length of stenosis was possible only in vessels with a diameter of at least 1.5 mm because vessels smaller than 1 mm in diameter exhibited very short stenosis (3–5 mm). Post-stenotic segments of 3–4 mm length could only be evaluated accurately for diameters down to 2 mm (Table 2).

Using the technique described above, vessel stenosis with a minimum diameter of 0.6 mm could be evaluated at 3T. MRI slightly overestimates the actual diameters (Table 4). The best results were obtained at a flow rate of 40 mL/min (Table 4). In the tests with NEX = 0.5, 1 and 2 did not produce any significant improvement in the results; the best signal-to-noise ratio could be obtained with the NEX = 2 method, and this didn't have any effect on the resolution (Table 5).

In the clinical situation, however, lower resolutions can be expected due to the limitations described previously. The flow rate had no statistically significant influence on the results. The best results could be obtained with a contrast medium concentration of 0.2 mmol/L, but a statistical correlation could not be verified. At 3.0T, the limits were reached with vessels of 1 mm and short stenosis of up to 5 mm in length. The post-stenotic area could only be evaluated in isolated cases (Table 2).

In a further step, the longitudinal imaging of stenotic and prestenotic vessel areas was investigated. This showed that exact longitudinal imaging is problematic, above all in vessel segments with diameters < 1 mm; in addition, mean variations of 0.72 mm with 1.5T and 0.58 mm with 3T were observed. The values for the variations in intrastenotic length measure-

Table 4. Spatial resolution 1.5 T and 3 T at a flow of 40 ml/min

Real diameter/mm	Diameter/mm measured at 1.5 T	Diameter/mm measured at 3.0 T
5.5	5.5	5.5
5	5	5.3
4.5	4.59	4.58
4	4.03	4
3.5	3.55	3.55
3	3.02	3
2.5	2.6	2.58
2	2.11	2.09
1.5	1.61	1.65
1	1.02	1
0.91	0.98	0.95
0.81		0.86
0.72		0.77
0.6		0.66

Table 5. Spatial resolution at 3 T in correlation to different flow velocity at NEX 2

Real diameter	Diameter measured at 40 ml/min	Diameter measured at 60 ml/min
5.5	5.5	5.62
5	5.3	5.29
4.5	4.58	4.62
4	4.0	4.10
3.5	3.55	3.65
3	3.0	3.12
2.5	2.58	2.61
2	2.09	2.15
1.5	1.65	1.160
1	1.0	1.09
0.91	0.95	0.99
0.81	0.88	0.91
0.72	0.77	0.81
0.6	0.66	0.69

ments shown in Fig. 3 are primarily due to high-grade stenosis of 79–90%. Since this concerns short narrowings of < 5 mm (Table 2), which are correspondingly difficult to image, this results in a substantial measurement error. With stenosis of < 70%, corresponding to vessel diameters of > 1 mm, the variation in measurement amounted to only 0.28 mm.

The values for the variations of the pre- and poststenotic segments were 0.53 mm in 1.5T and 0.58 mm in 3T (Fig. 4).

4. Discussion

With the present 3.0T scanner hardware, software, and sequences, in vitro 3D coronary MRI with a high SNR and an enhanced spatial resolution has been demonstrated to be feasible. So far, only one group has investigated the possibilities for in vivo 3T MRA of coronary arteries. A clear improvement in coronary imaging, with respect to longitudinal imaging, could be achieved in healthy adult subjects (15).

Furthermore, an improvement was possible in SNR and CNR compared with the corresponding sequence at 1.5T (22). The sharpness of the coronary vessels was comparable at both field strengths (vessel sharpness 24–49% vs. 46% ± 10). With these results, it is necessary to take into account that the tests at 3T were carried out on healthy volunteers, and it might not be so easy to transfer the method to measurements in patients (15, 23).

Actually, there is no study available on the use of high-field equipment > 3T in clinical situations.

In 2001, Dougherty et al. investigated the effect of field strength on SNR. This could be increased 2.0-fold at 3T and 2.5-fold at 4T as compared to 1.5T (9, 16). This improvement can be used to increase in-plane resolution as well as to reduce layer thickness and the time needed for the test (16) (Figs. 7 and 8).

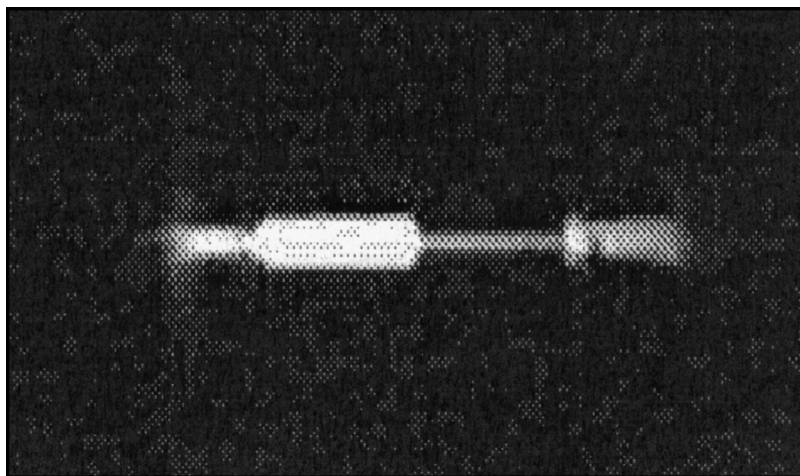


Figure 7. 3 T MRI. Vessel phantom with 0.8 mm diameter. The degree and the length of the stenosis is clearly visible.

In this study, high-field MRI showed a clearly better imaging of the stenosis morphology. Compared to MRI at 1.5T, a higher spatial resolution was possible with the 3 D scanner. With the 3T MRI scanner, it is possible to image stenosis down to a diameter of 0.60 mm compared to diameter of 0.91 mm with 1.5T MRI. The length of stenosis were assessed with a higher accuracy at 3T (Fig. 3, Table 4).

The best signal-to-noise ratio was obtained with the NEX = 2 method, and this had no effect on the resolution. The resolution capacity of the MR method is also dependent on the length of the stenosis. Currently, the limits with short stenosis of 5 mm are 1 mm, compared to 0.6 mm with long narrowings of 7–11 mm. This is also reflected in the measurement error, which is clearly higher in vessels < 1 mm (Fig. 3). It is precisely with high-grade and short stenosis that the advantage of high-field MR imaging becomes apparent since these cannot be adequately imaged with a conventional scanner at up to 1.5T.

The disadvantages of high-field MR imaging so far established, e.g. decreased $T2^*$ times and increased B_0 effects, could not be observed in this study.

The flow rate had no influence on the results. The effect of the concentration of contrast medium was not statistically verifiable in the same tests. This represents a limitation of the in vitro data in regarding to the brief concentration of contrast medium in coronary vessels in case of using the available contrast medium. Future use of blood-pool contrast media holds a promise of improved results.

An important limitation of these in vitro studies is that 3-dimensional cardiac and respiratory movements have not been considered in the test results.

There is a substantial difference in signal between 1.5T and 3T in the dephasing experienced by the spins as a result of inhomogeneities in the magnetic field. The effective relaxation time, $T2^*$, which in addition to T2 includes the effects of inhomogeneities in the magnetic field, is clearly shorter than

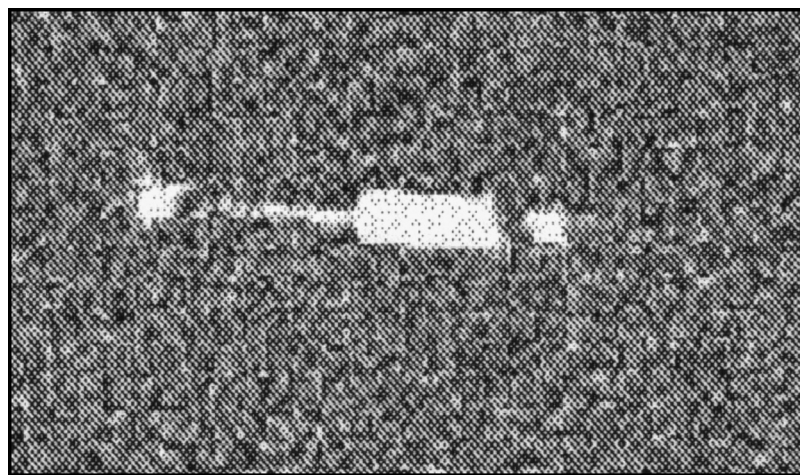


Figure 8. 1.5 T MRI. Vessel phantom with 0.8 mm diameter. The degree and the extent of the stenosis is not assessable due to the spatial resolution.

at 1.5T. This increases the influence of susceptibility artefacts. This can, however, be partially decreased again by an increase in spatial resolution or by the selection of thinner layers, but at the expense of a reduced SNR. Compared to 1.5T, the increased sensitivity to inhomogeneities in the magnetic field leads to a reduction in signal intensity for gradient sequences at the same echo time. Furthermore, the substantially higher dephasing due to the field inhomogeneities leads to an increase in extinction and distortion effects. This effect can be reduced by a reduction in the number of Fourier lines taken up by the echo train, which can, for example, be effected through segmentation of the k space or by parallel imaging.

The clear increase in SNR at 3T raises the possibility that in the future fine anatomical details such as the chorda tendinae and mitral valve leaflets can be recognized (24); hence, an increase in the range of indications seems to be a possibility (25). Further improvements in data acquisition can be achieved through the use of steady-state free precession (SSFP) technology (11).

There is no cause for concern about effects on vital signs or about any danger to patients. In a study on healthy volunteers up to a maximum 8T, Chakeras et al. were able to observe only a slight increase of 3.6 mmHg in systolic blood pressure (26).

Due to the potentially high resolution of up to 0.6 mm, it can be expected that it will be possible to image the distal vessel segments, which so far have been excluded from MRI. Whether high-field Magnetic resonance coronary angiography (MRCA) will also be able to identify short, high-grade stenosis in distal segments cannot currently be assessed with certainty. However, in the near future this will certainly remain within the domain of cardiac catheterization investigations while MRCA appears to be eminently suitable for risk evaluation and for the planning of interventional procedures.

The results of the study show that MRCA at 3T is possible and that a substantial improvement in results can be expected. Further improvements to the hardware as well as a better depth adaptation of the sequences by means of altered basic physical parameters are necessary (15). In the present study, feasibility and spatial resolution were tested.

As a next step, it is planned to perform tests on native vessel preparations in order to confirm the improved spatial resolution and SNR in the evaluation of vessel stenosis. If the encouraging results thus far are confirmed, further comparative studies at 1.5 and 3T in healthy volunteers and in patients with coronary artery disease will be possible in order to evaluate the use of the method in daily clinical practice.

Future developments and enhancement of high-field MRI promise better lumen and coronary artery wall imaging and this may become a new target in noninvasive evaluation of CAD.

References

1. McConnell MV, Khasgiwala VC, Savorg BJ, Chen MH, Chuang ML, Edelman RR, Manning WJ. Prospective adaptive navigator correction

- for breath-hold MR coronary angiography. *Magn Reson Med* 1997; 37:148–152.
2. Wittlinger T, Voigtländer T, Rohr M, Meyer J, Thelen M, Kreitner KF, Kalden P. Magnetic resonance imaging of coronary artery occlusions in the navigator technique. *Int J Card Imaging* 2002; 18: 203–211.
3. Müller MF, Fleisch M, Kroeker R, Chatterjee T, Meier B, Vock P. Proximal coronary artery stenosis: three-dimensional MRI with fat saturation and navigator echo. *JMRI* 1997; 7:644–651.
4. Pennel DJ, Keegan J, Firmin DN, Gatehouse PD, Underwood SR. Magnetic resonance imaging of coronary arteries: techniques and preliminary results. *Br Heart J* 1993; 70:315–326.
5. Post JC, van Rossum AC, Hofman MB, Visser CA. Three-dimensional respiratory-gated MR angiography of coronary arteries: comparison with conventional coronary angiography. *AJR Am J Roentgenol* 1996; 166:1399–1404.
6. Stuber M, Botnar RM, Danias PG, Sodickson DK, van Cauteren M, de Becker J, Manning WJ. Double-oblique free-breathing high-resolution three-dimensional coronary magnetic resonance angiography. *AJR Am J Roentgenol* 1999; 34:524–531.
7. Nagel E, van Rossum AC, Fleck E. *Kardiovaskuläre Magnetresonanztomographie*. 1. Ausgabe. Darmstadt: Steinkopff Verlag, 2002.
8. Kim WY, Danias PG, Stuber M, Flamm SD, Plein S, Nagel E, Langerak SE, Weber OM, Pedersen EM, Schmidt M, Botnar RM, Manning WJ. Coronary magnetic resonance angiography for the detection of coronary stenoses. *N Engl J Med* 2001; 345:1863–1869.
9. Baudienstiel KT, Heverhagen JT, Knopp MV. Klinische MRT bei 3 Tesla: Aktueller Stand. *Radiologe* 2004; 44:11–18.
10. Chakeras DW, Kangarlu A, Boudoulas H, Young DC. Effect of static field exposure of up to 8T on sequential human vital sign measurements. *J Magn Reson Imaging* 2003; 18:346–352.
11. Schar M, Kozerke S, Fischer SE, Boesiger P. Cardiac SSFP imaging at 3T. *Magn Reson Med* 2004; 51:799–806.
12. Voigtländer T. *Habilitationsschrift des Fachbereiches Medizin der Johannes Gutenberg: Universität Mainz*, 2000.
13. Noeske R, Seifert F, Rhein KH, Rinnberg H. Human cardiac imaging at 3T using phased array coils. *Magn Reson Med* 2000; 44:978–982.
14. Atalay MK, Poncelet BP, Kantor HL, Brady TJ, Weisskopf RM. Cardiac susceptibility artifacts arising from the heart-lung interface. *Magn Reson Med* 2001; 45:341–345.
15. Stuber M, Botnar RM, Fischer SE, Lamerichs R, Smink J, Harvey P, Manning WJ. Preliminary report on in vivo coronary MRA at 3 Tesla in humans. *Magn Reson Med* 2002; 48:425–429.
16. Dougherty L, Connick TJ, Mizsei G. Cardiac imaging at 4T. *Magn Reson Med* 2001; 45:176–178.
17. Danias PG, Manning WJ. Coronary MR angiography: current status. *Herz* 2000; 25:431–439.
18. Stuber M, Botnar RM, Danias PG, Dodickson DK, Kissinger KV, Van Cauteren M, De Becker J, Manning W. Double oblique free-breathing high-resolution 3D coronary MRA. *J Am Coll Cardiol* 1999; 34:524–531.
19. Hoogeveen RM, Bakker CJG, Mall W, Viergever MA. Vessel diameter measurements in TOF and PC angiography: a need for standardization. In: *Proceedings of the 5th Meeting of the ISMRM*. Vol 1. 1997: 1847.
20. Lin LI. A concordance correlation coefficient to evaluate reproducibility. *Biometrics* 1989; 45:255–268.
21. *Wissenschaftliche Tabellen Geigy, Teilband Statistik*, 8. Auflage 1980, Nachdruck 1985, Seite 224.
22. Gutberlet M, Spors B, Grothoff M, Freyhardt P, Schwinge K, Plotkin M, Amthauer H, Noeske R, Felix R. Comparison of different cardiac MRI sequences at 1.5T/3.0T respect to signal-to-noise and contrast-to-noise ratios—initial experience. *Rofo Fortschr Geb Roentgenstr Neuen Bildgeb Verfahren* 2004; 176:801–808.

23. Stuber M, Danias PG, Botnar RM, Sodickson DK, Kissinger KV, Manning WJ. Superiority of prone position in free-breathing 3D coronary MRA in patients with coronary artery disease. *J Magn Reson Imaging* 2001; 13:185–191.
24. Hinton DP, Wald LL, Pitts J, Schmitt F. Comparison of cardiac MRI on 1.5 and 3.0 Tesla clinical whole body systems. *Invest Radiol* 2003; 38:436–442.
25. Leiner T, de Vries M, Hoogeveen R, Vasbinder GB, Lemaire E, van Engelshoven JM. Contrast-enhanced peripheral MR angiography at 3 Tesla: initial experience with a whole-body scanner in healthy volunteers. *J Magn Reson Imaging* 2003; 17:609–614.
26. Kangarlu A, Baudenstiel KT, Heverhagen JT, Knopp MV. Klinische Hoch- und Ultrahochfeld-MR und Ihre Wechselwirkung mit biologischen Systemen. *Radiologe* 2004; 44:19–30.